

Stellar populations in the outskirts of spiral galaxies using IFU CALIFA data

**T. Ruiz-Lara¹, E. Florido^{1,2}, I. Pérez^{1,2}, P. Sánchez-Blázquez³,
J. Falcón-Barroso^{4,5}, and R. Cacho⁶**

¹ Dpto. de Física Teórica y del Cosmos, Universidad de Granada, Facultad de Ciencias (Edificio Mecenaz), 18071 Granada, Spain. e-mail: ruizlara@ugr.es

² Instituto Universitario Carlos I de Física Teórica y Computacional, Universidad de Granada, 18071 Granada, Spain

³ Dpto. de Física Teórica, Universidad Autónoma de Madrid, E-28049 Cantoblanco, Spain

⁴ Instituto de Astrofísica de Canarias (IAC), La Laguna, S/C de Tenerife, Spain

⁵ Dpto. Astrofísica, Universidad de La Laguna (ULL), 38206 La Laguna, Tenerife, Spain

⁶ Dpto. de Astrofísica y CC. de la Atmósfera, Universidad Complutense de Madrid

Abstract

We present a project to study the stellar populations in the outskirts of spiral galaxies. We analyse the possible different radial mixing processes characterising different luminosity profiles and morphologies. This study makes use of the IFU spectroscopic data of the CALIFA collaboration. We have selected a sample of around 60 spiral galaxies from the CALIFA sample. This survey is providing us with unprecedented data which allow us to obtain stellar parameters and break the age-metallicity degeneracy up to large galactocentric radii. In addition, we are characterising the radial surface brightness and colour profiles of the galaxies in the g , r and i SDSS bands. In this work we study five galaxies with different luminosity profiles. We confirm that we can successfully obtain information about the stellar population in the outer parts of the galaxies. So far, we find no differences in the stellar age and metallicity distributions between barred and unbarred galaxies or among different surface brightness profile types.

1 Introduction

Pioneering works [16, 11] described the radial light distribution in spiral galaxies as an exponential, as the result of the angular momentum conservation during the galaxy formation [7]. With the advent of bigger telescopes and better instruments we can reach and study the outer parts of galaxies. Two important features deviate from this exponential profiles in the outer parts: truncations and breaks [14]. The truncation of stellar discs was first shown by

[31], who found that this exponential profile does not extend to an arbitrarily large radii and it has a relatively sharp edge in the surface brightness distribution. Several recent studies have dealt with these profiles [8, 9] not only in the local universe, but also at high redshift [18, 30]. Sometimes truncations have been confused with breaks. We can define breaks in the profiles as changes in the exponential slope, resulting in an inner and outer slope ([21], PT06 hereafter). PT06 have identified three basic types of profiles attending to breaks: 1) the pure exponential profiles (type I) with no breaks, 2) type II with a *downbending break*, and 3) type III, also described by a broken exponential but with an *upbending* profile. At these large radii, the gas density is well below the threshold of star formation ($10 M_{\odot} \text{ pc}^{-2}$) and thus the presence of stars is not well understood.

Despite the heavy efforts showed in the last few years to characterise disc profiles, little is still known about the properties and origin of these outer discs. The most plausible causes to explain these profiles are the angular momentum conservation [32] and star formation threshold [13]. An insight into the properties of the stars that populate these regions and comprehensive models of galactic formation can help to discern among the different physical processes that have built the outer discs.

Only a few studies have looked into the stellar populations properties of the outer discs. [9] showed the dependence of the truncation radius with wavelength, being larger for shorter wavelengths. Other studies have used colour profiles (e.g. [6, 2]) showing negative age gradients or evidences of *U-shape* in the age profiles. Very few studies are starting to use Integral Field Spectroscopic (IFS) data [34] to obtain stellar parameter trends; they find *U-shape* age distribution in some type II galaxies. On the modelling side, recent works [23, 15] suggest stellar migration as the cause of some of the characteristics observed in the stellar surface brightness and stellar population profiles in the discs. [23] predicted, using numerical simulations that: 1) disc galaxies should have exponential surface brightness profiles beyond the break radius, and 2) disc galaxies should have a radial age profile with an *U-shape*, with younger stars located at the break position. [28] suggest that breaks and the corresponding *U-shape* in age profiles are due to a different rate of star formation between the inner and the outer parts of the galaxy. A magnetic effect could also be responsible for this stellar migration [3].

In this pilot work we study the outer part of 5 spiral galaxies using IFS data. This is part of a project aiming at disentangling the nature of the breaks and truncations in the surface brightness radial profiles of spiral galaxies.

2 Sample and data characterization

We have selected a subsample of 60 galaxies from the CALIFA sample based on the Hyperleda catalogue [17]. These are spiral galaxies ($0 \leq T \leq 8$), with low to intermediate inclinations ($0^{\circ} \leq i \leq 75^{\circ}$) and small enough to fit the outer parts of the galaxies within the limited PMAS-PPAK field of view ($d_{25} < 95''$). Moreover, we have visually inspected them in order to avoid signs of strong interaction. We select a pilot sample for this study of five galaxies covering the different surface brightness (SB) profile types (see Table 1).

Table 1: Sample properties: (1), (2), (3), (4) and (5) were taken from Hyperleda [17] while (6), (7), (8) and (9) were obtained with our ellipse fitting procedure. h is the inner disc scale-length in SDSS r -band.

Galaxy	RA	DEC	Morphological	v	i	h	Profile	R_{Break}
	J2000	J2000	type	(km s ⁻¹)	(°)	(")	type	(")
(1)	(2)	(3)	(4)	(5)	(6)	(7)	(8)	(9)
NGC 0001	00:07:15.9	+27:42:29.1	Sb	4540.9	46.52	12.46	III	40.49
NGC 0496	01:23:11.6	+33:31:45.4	Sbc	6012.0	57.86	15.58	II	40.26
UGC 03944	07:38:36.5	+37:38:00.6	Sc	3904.7	33.59	15.53	II	44.43
UGC 05108	09:35:26.3	+29:48:45.4	SBab	8127.9	65.35	10.71	I	–
NGC 5947	15:30:36.0	+42:43:01.0	SBbc	5890.9	62.99	12.48	II	30.21

We use the CALIFA spectroscopic data [26] to study the stellar population in these galaxies. These data are being taken with the PMAS/PPAK integral field spectrophotometer [24]. This instrument has a field of view of $74'' \times 64''$ and 331 fibers with a diameter of $2.7''$ and a covering factor of 100% due to a three position dithering pattern. The spectra cover the range $\lambda\lambda 3400\text{--}4750 \text{ \AA}$ with the V1200 grating (FWHM $\sim 2.7 \text{ \AA}$, exposure time ~ 90 minutes) and $\lambda\lambda 3745\text{--}7300 \text{ \AA}$ with the V500 (FWHM $\sim 6 \text{ \AA}$, exposure time ~ 45 minutes). Standard data reduction procedures are carried out by the CALIFA pipeline [12].

We use the SDSS DR7 data [1] to obtain the SB profiles. SDSS is observing with a field of view of $13.5' \times 9.8'$, exposure time of 53.9 s and a pixel size of $0.396''$. SDSS pipeline applies a bias subtraction and flat-field correction to these data. Sky subtraction is not applied by this pipeline, which allows us to obtain an improved sky subtraction. We compute the median flux value in tens of boxes with different sizes around the galaxies far enough of strong light sources. We carry out a $3\text{-}\sigma$ clip to discard outliers. The mean value is assumed to be the sky value (e.g. [21]). With this sky subtraction we can reach 28 mag arcsec⁻² in r band, 1 mag arcsec⁻² deeper than with the DR8 which uses its own sky subtraction scheme.

3 Methodology

We apply the `ellipse IRAF`¹ task to the SDSS DR7 frames to obtain the one-dimensional SB distribution. To avoid contamination by point-like sources, we mask these SDSS images. For the fitting, first we fix the centre and allow the ellipticity (e) and the position angle (PA) to vary. This type of fitting is sensitive to morphological features. After finding the outer e and PA (disc), we fix both parameters and another set of ellipses are fitted, sensitive to the underlying disc light distribution. We define the break position as the point in which both exponential fittings intersect each other (Fig. 1).

Concerning the stellar parameters, we use the PINGSOFT package for IFS visualisation

¹IRAF is distributed by the National Optical Astronomy Observatory, which is operated by the Association of Universities for Research in Astronomy (AURA) under cooperative agreement with the National Science Foundation.

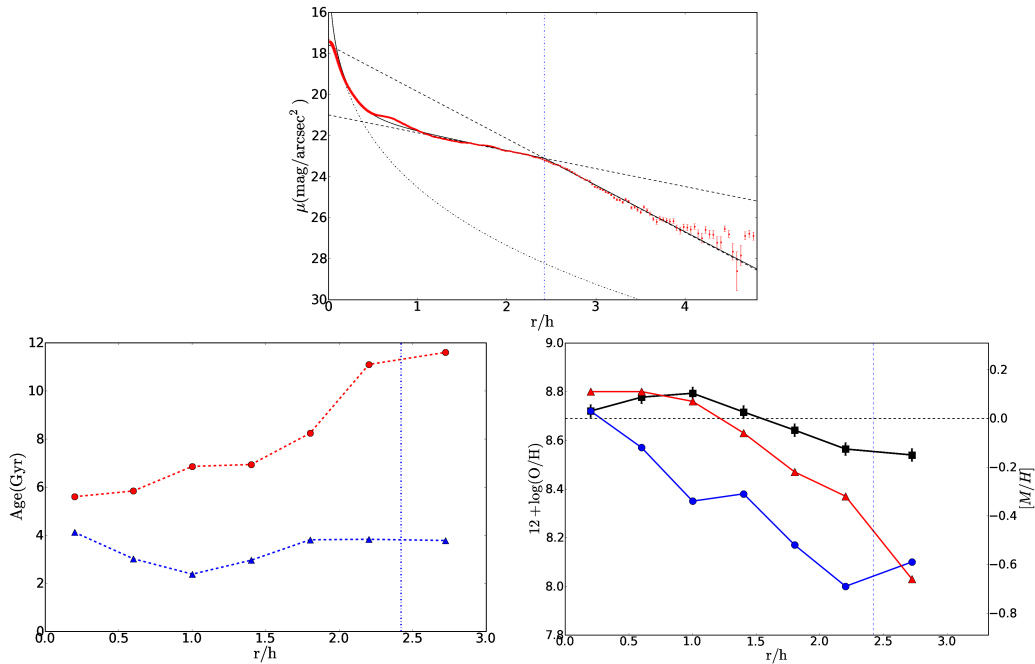


Figure 1: NGC 5947 is an example of galaxy in which we reach beyond the break radius. *Up*: r -band surface brightness profile and bulge-disc decomposition. *Bottom left*: age profile. *Bottom right*: comparison between stellar metallicity and gas abundance gradients (black squares). Vertical dashed blue lines are located at the break radius, blue and red symbols represent luminosity and mass-weighted parameters respectively.

and analysis [22] to extract spectra at different radii integrating over elliptical apertures from the CALIFA V500 data. That allows us to obtain spectra with a S/N of around 50 in the $H\beta$ region required to determine reliable stellar parameters [29]. With these data we study the stellar population up to 3 disc scale-lengths reaching $24 \text{ mag arcsec}^{-2}$ in r band.

We remove the emission lines from the gaseous components with GANDALF [25]. It treats the emission lines as additional Gaussian templates and uses the penalised pixel-fitting pPXF [4] code to find the best combination of velocities, velocity dispersions and stellar templates. We use the models of [33] based on the MILES library² [27] as templates. In this way we can obtain the shape and the flux of the observed emission lines.

We use STARLIGHT [5] to obtain the stellar parameters. This code is able to decompose an observed spectrum in a superposition of single stellar populations (SSP) of various ages and metallicities. We derive the star formation histories of galaxies and other quantities such as the mean stellar age and metallicity and $[\alpha/\text{Fe}]$ enhancement.

Using the emission spectrum fitted by GANDALF we can obtain information about the interstellar medium (ISM). We have studied gas abundances by means of the O3N2 abundance indicator [20] following the methodology described in [10]. In this way, we obtain information

²The model are publicly available at <http://miles.iac.es>

about both the stellar properties and the present-day gaseous abundances.

4 Results and conclusions

In this work we have analysed the SB profiles, the distribution of stellar age and metallicity as well as gas abundances gradients for a pilot sample of five galaxies. We can study the stellar populations up to 3 disc scale-lengths reaching 24 mag arcsec⁻² in r band, which means study the outer parts. Therefore, we have demonstrated the feasibility of this project with this kind of data.

We find a variety of behaviours in the five galaxies, however our sample is too small to draw any firm conclusions. In addition, we encountered differences in the distribution of luminosity-weighted (more sensitive to the last star burst) and mass-weighted (sensitive to old stars) stellar parameters.

In general terms, we find no differences in the stellar age and metallicity distributions between barred and unbarred galaxies or between different SB profile types. We find negative stellar metallicity gradients in agreement with other studies [29] and models [28, 23]. Some stellar age profiles show negative gradients (UGC 03944 and UGC 05108) while others show some evidences of an *U-shape* (NGC 0001, NGC 0496 and NGC 5947), according to recent works [34].

If we compare the gas abundance gradients and the distribution of stellar metallicity we can find shallower gradients for the ionised gas than for the stars. In addition, the gas is usually more metal rich than the stars as a consequence of the ISM enrichment due to the stellar evolution.

In Fig. 1, we show stellar age and metallicity profiles for NGC 5947 as an example. For this type II galaxy we find negative gradients in the stellar metallicity and gas abundance distributions, and the characteristic *U-shape* for the luminosity-weighted stellar age gradient, although we find a positive gradient in the case of mass-weighted stellar age. The stellar metallicity of this galaxy is higher than the gas abundance in the centre (see also [10]). The strange behaviour of the mass-weighted stellar age distribution still remain to be clarified.

To summarise, we have studied a pilot sample of five galaxies. This sample is too small to draw any conclusions. As future work, we will obtain stellar and gas properties as well as star formation histories at different radii for 60 galaxies, which will allow us to clarify the nature of the outer parts of spiral galaxies.

Acknowledgments

We acknowledge the usage of the HyperLeda database (<http://leda.univ-lyon1.fr>). TRL thanks the support of the Spanish Ministerio de Educación, Cultura y Deporte by means of the FPU fellowship. TRL also wants to thank the organiser of the X Scientific Meeting of the Spanish Astronomical Society for the grant for accommodation. This research has been supported by the Spanish Ministry of Science and Innovation (MICINN) under grants AYA2011-24728, AYA2007-67625-C02-02 and Consolider-Ingenio CSD2010-00064; and by the Junta de Andalucía (FQM-108).

References

- [1] Abazajian, K. N., et al. 2009, *ApJS*, 182, 543
- [2] Bakos, J., Trujillo, I., & Pohlen, M. 2008, *ApJ*, 683, L103
- [3] Battaner, E., Florido, E., Guijarro, A., & Jiménez-Vicente, J. 2002, *A&A*, 338, 213
- [4] Cappellari, M. & Emsellem, E. 2004, *PASP*, 116, 138
- [5] Cid Fernandes, R., Mateus, A., Sodré L., Stasińska, G., & Gomes, J. M. 2005, *MNRAS*, 358, 363
- [6] de Jong, R.S. 1996, *A&A*, 313, 377
- [7] Fall, S. M. & Efstathiou, G. 1980, *MNRAS*. 193, 189
- [8] Florido, E., Battaner, E., Guijarro, A., Garzón, F., & Castillo-Morales, A. 2006, *A&A*, 455, 467
- [9] Florido, E., Battaner, E., Zurita, A., & Guijarro, A. 2007, *A&A*, 472, 39
- [10] Florido, E., Pérez, I., Zurita, A., & Sánchez-Blázquez, P. 2012, *A&A*, 543, 150
- [11] Freeman, K. C. 1970, *ApJ*, 160, 811
- [12] Husemann, B., et al., 2012, submitted
- [13] Kenicutt, R. C. Jr. 1989, *ApJ*, 344, 685
- [14] Martín-Navarro, I., Bakos, J., Trujillo, I., et al. 2012, *MNRAS*, 427, 1102
- [15] Martínez-Serrano, F. J., Serna, A., Domínguez-Tenreiro, R., & Mollá, M. 2008, *MNRAS*, 388, 39
- [16] Patterson, F. S. 1940, *Harvard Coll. Obs. Bull.*, 914, 9
- [17] Paturel, G., Petit, C., Prugniel, Ph., et al. 2003, *A&A*, 412, 45
- [18] Pérez, I. 2004, *A&A*, 427, 17
- [19] Pérez, I. & Sánchez-Blázquez, P. 2011, *A&A*, 529, A64
- [20] Pettini, M. & Pagel, B. E. J. 2004, *MNRAS*, 348, L59
- [21] Pohlen, M. & Trujillo, I. 2006, *A&A*, 454, 759
- [22] Rosales-Ortega, F. F. 2011, *NewA*, 16, 220
- [23] Roskar, R., Debattista, V. P., Stinson, G. S., et al. 2008, *ApJ*, 675, L65
- [24] Roth, M. M., Kelz, A., Fechner, T., et al. 2005, *PASP*, 117, 620
- [25] Sarzi, M., Falcón-Barroso, J., Davies R. L., et al. 2006, *MNRAS*, 366, 1151
- [26] Sánchez, S. F., Kennicutt, R. C., Gil de Paz, A., et al. 2012, *A&A*, 538, A8
- [27] Sánchez-Blázquez, P., Peletier, R., Jiménez-Vicente, J., et al. 2006, *MNRAS*, 371, 703
- [28] Sánchez-Blázquez, P., Gibson, B. K., Courty, S., & Brook, C. 2009, *MNRAS*, 398, 591
- [29] Sánchez-Blázquez, P., Ocvirk, P., Gibson, B. K., Pérez, I., & Peletier, R. F., 2011, 415, 709
- [30] Trujillo, I. & Pohlen, M. 2005, *ApJ*, 630, L17
- [31] Van der Kruit, P. C. 1979, *A&A*, 38, 15
- [32] Van der Kruit, P. C. 1987, *A&A*, 173, 59
- [33] Vazdekis, A., Sánchez-Blázquez, P., Falcón-Barroso, J., et al. 2010, *MNRAS*, 404, 1639
- [34] Yoaquim, P., Roskar, R., & Debattista, V. 2012, *ApJ*, 752, 97